www.sciencetranslationalmedicine.org/cgi/content/full/7/292/292ra99/DC1

Supplementary Materials for

Vinculin network–mediated cytoskeletal remodeling regulates contractile function in the aging heart

Gaurav Kaushik, Alice Spenlehauer, Ayla O. Sessions, Adriana S. Trujillo, Alexander Fuhrmann, Zongming Fu, Vidya Venkatraman, Danielle Pohl, Jeremy Tuler, Mingyi Wang, Edward G. Lakatta, Karen Ocorr, Rolf Bodmer, Sanford I. Bernstein, Jennifer E. Van Eyk, Anthony Cammarato,* Adam J. Engler*

*Corresponding author. E-mail: acammar3@jhmi.edu (A.C.); aengler@ucsd.edu (A.J.E.)

Published 17 June 2015, *Sci. Transl. Med.* **7**, 292ra99 (2015)
DOI: 10.1126/scitranslmed.aaa5843

This PDF file includes:

Other Supplementary Material for this manuscript includes the following:

(available at www.sciencetranslationalmedicine.org/cgi/content/full/7/292/292ra99/DC1)

Table S1 (Microsoft Excel format). Peptides detected by mass spectroscopy for adult and aged rhesus monkey left ventricles.
Table S2 (Microsoft Excel format). Peptides detected by mass spectroscopy for adult and aged rat left ventricles.
Table S3 (Microsoft Excel format). Proteomic analysis for adult and aged rhesus monkey left ventricles.
Table S4 (Microsoft Excel format). Proteomic analysis for adult and aged rat left ventricles.
Table S5 (Microsoft Excel format). STRAP annotation of the cellular compartments of proteins detected in both rat and monkey proteomes.
Table S6 (Microsoft Excel format). STRAP annotation of biological functions for rat and monkey.
Table S7 (Microsoft Excel format). IPA of bio-function expression for rat.
Table S8 (Microsoft Excel format). IPA of tox-function expression for rat.
Table S9 (Microsoft Excel format). IPA and OMIM annotation of age–up-regulated proteins associated with cardiac function.
Table S10 (Microsoft Excel format). IPA of upstream regulators of age-related proteins identified in rat and simian.
Table S11 (Microsoft Excel format). Expression of candidate actin-binding molecules in *Drosophila* hearts using qPCR.
Table S12 (Microsoft Excel format). Fitting shortening velocities with Hill's muscle model.
Table S13 (Microsoft Excel format). qPCR primers.

MATERIALS AND METHODS

Proteomic analysis of ventricular tissue

Heart tissues were solubilized in 8 M urea, 2 M thiourea, 4% CHAPS, and 1% dithiothreitol, and centrifuged at 16,000 rpm for 20 min. Protein concentration of the supernatant was determined by CB-X assay kit (G-Biosciences). One-hundred μg of protein was reduced, alkylated, and digested with trypsin using FASP protein digest kit (Expedeon). Peptides were desalted using Oasis HLB 96-well Plate (Waters). Two μg of peptides were analyzed using label-free quantification on a reversed-phase liquid chromatography tandem mass spectrometry (RPLC–MS/MS) online with an Orbitrap Elite mass spectrometer (Thermo Scientific) coupled to an Easy-nLC 1000 system (Thermo Scientific). Peptides were concentrated on a C18 trap column (Acclaim PepMap 100, 300 μm × 5 mm, C18, 5 μm, 100 Å; maximum pressure 800 bar) in 0.1% aqueous trifluoroacetic acid, then subsequently separated on a C18 analytical column (Acclaim PepMap RSLC, 75 μm × 15 cm, nano Viper, C18, 2 μm, 100 Å) using a linear gradient from 5% to 35% solvent B over 155 min (solvent A: 0.1% aqueous formic acid and solvent B: 0.1% formic acid in acetonitrile; flow rate 350 nl/min; column oven temperature 45°C). The analysis was operated in a data-dependent mode with full scan MS spectra acquired at a resolution of 60,000 in the Orbitrap analyzer, followed by tandem mass spectra of the 20 most abundant peaks in the linear ion trap after peptide fragmentation by collision-induced dissociation (CID).

Database searching and processing

Tandem mass spectrometry analysis was performed as published previously (*47*). All raw MS/MS data obtained from the Orbitrap Elite were converted to mzXML and mgf format using Msconvert version 3.0.3858 from ProteoWizard for peaklist generation. All data were searched using two search engines: X!Tandem algorithm version 2009.10.01.1 and OMSSA algorithm version 2.1.9. Rat Heart dataset was searched against the concatenated target/decoy Rat Uniprot database as of May 16, 2013, and the Monkey Heart dataset was searched against the concatenated target/decoy Human Uniprot database as of April 22, 2013. The search parameters were as follows: fixed modification of Carbamidomethyl (C) and variable modifications of Oxidation (M), Phosphorylation (STY); Enzyme:

Trypsin with two maximum missed cleavages; Parent Tolerance: 0.01 Da for Rat Heart dataset and 0.08 Da for Monkey Heart dataset; Fragment tolerance: 1.00 Da. Post-search analysis was performed using Trans Proteomic Pipeline version 4.6, rev 1 with protein group and peptide probability thresholds set to 90% and 90%, respectively, and one peptide required for identification. PeptideProphet was used for peptide validation and iProphet was used to further refine the identification probabilities. Lastly, ProteinProphet was then used to infer protein identifications from the resulting combined peptide list and perform grouping of ambiguous hits.

Protein isoforms were only used if a peptide comprising an amino acid sequence that was unique to the isoform was identified. Uncharacterized or unknown proteins were blasted again "all" mammalian database to infer a common protein name if the amino acid sequence matched 100%. Spectra of proteins identified based on a single peptide were manually validated. Protein Group and Peptide False Discovery Rates were calculated automatically using a target-decoy method for the above probability thresholds (1.28 and 0.18%, respectively, for Rat Heart dataset, and 1.64 and 0.27%, respectively, for Monkey Heart dataset). The final non-redundant protein lists were analyzed through the use of IPA (Ingenuity Systems), when isoforms were observed, peptides comprising amino acid sequence unique to each isoform were noted. Networks and functional and pathway analyses were performed with IPA, Software Tool for Rapid Annotation of Proteins (STRAP), and/or Online Mendelian Inheritance in Man (OMIM) as indicated.

Adult rat echocardiography

Each rat was placed on an IACCUC-approved heating pad and anesthetized with 1.5% isofluorane in 100% O_2 by facemask. Echocardiographic images were obtained using a GE vivid/I imaging system. Echocardiography was performed to measure systolic and diastolic left ventricular (LV) dimensions, mass, and percent fractional shortening from motion-mode kymographs. The entire procedure was approximately 30 min in length per animal. Animals regained full consciousness at the end of procedure and are transferred to cages. Echocardiography was performed within 1 week of sacrifice and heart tissue isolation.

Histology and immunofluorescence of rat myocardium

Each heart was sectioned using a Cryocut 1800 (Leica) in 10-μm slices and stored at -80^{o}C until staining. Each slice was fixed with 3.7% formaldehyde in PBS and then blocked with staining buffer (0.3% Triton-100X, 2% w/v ovalbumin in PBS). Samples were incubated in primary antibody (1:1000 Sigma Aldrich mouse anti-vinculin, 1:1000 Sigma Aldrich rabbit anti-Cnx43) in staining buffer, washed, incubated in secondary antibody (1:1000 CY5 goat anti-mouse, 1:1000 FITC donkey anti-rabbit, 1:1000 phalloidin) in staining buffer, washed, incubated in Hoechst (1:10,000) in staining buffer, washed, and finally mounted with fluoromount and a plastic coverslip. Imaging was performed using a Zeiss LSM 780 Laser Scanning Confocal Microscope.

To analyze vinculin localization within the cell, Cnx43-positive pixels were used a region of interest (ROI) mask to mark the intercalated discs, since Cnx43 is only expressed at this location. In this way, we can associate vinculin-indicating fluorophores with the intercalated disc (via Cnx43). Vinculin-colocalized pixels were identified using the Pearson's colocalization analysis (in which a value of -1 indicates no colocalization between fluorophores and +1 indicates perfect colocalization) (*65*) using ImageJ-based FIJI software. The calculated thresholding value for vinculin/Cnx43 colocalization fluorescence was then used to separate the vinculin channel into Cnx43 co-localized (intercalated disc) and non-Cnx43 co-localized pixels (interpreted as cortical) in a custom-built Matlab code (see below). Integrated density was measured as total grey value per frame divided by the number of vinculin-positive pixels. The DAPI channel was used as an internal normalization control, where DNA was labeled using 1:10,000 Hoechst (fig. S4).

```
function [Result] = Colocalize_CM(cnx,vinc,dapi,thresh)

% cnx is an image of cnx fluorescence
% vinc is an image of vinculin fluorescence
% dapi is an image of dapi/nucleui fluorescence
cnx = double(cnx);
vinc = double(vinc);
dapi = double(dapi);

dims = size(vinc);
rows = dims(1);
```

```
cols = dims(2);

% Set min to zero
minput_v = min(min(vinc));
minput_c = min(min(cnx));
minput_d = min(min(dapi));

for r = 1:rows
   for c = 1:cols
      vinc(r,c) = vinc(r,c) - minput_v;
      cnx(r,c) = cnx(r,c) - minput_c;
      dapi(r,c) = dapi(r,c) - minput_d;
   end
end

% NORMALIZATION
% Normalize so matrices run from 0 to 1
max_cnx = max(max(cnx));
max_vinc = max(max(vinc));
max_dapi = max(max(dapi));
cnx = cnx./max_cnx;
vinc = vinc./max_vinc;
dapi = dapi./max_dapi;
max_cnx = max(max(cnx));
max_vinc = max(max(vinc));
max_dapi = max(max(dapi));

Result.cnx = cnx;
Result.vinc = vinc;
Result.dapi = dapi;

% These counters count up the number of pixels in which Vinculin and
% Connexin colocalize above a given threshold (thresh) which is a
% fraction of the maximal Connexin intensity
coloc_counter = 0;
nocoloc_counter = 0;
coloc_intensity = 0;
nocoloc_intensity = 0;

% Will threshold for colocalization above a certain amoutn
thresh_cnx = thresh*max_cnx;
thresh_vinc = thresh*max_vinc;
thresh_dapi = thresh*max_dapi;

% Will populate with pixels for colocalization
coloc_matrix = zeros(rows,cols);
```

```
coloc_histo = [];
% Will populate with pixels where Vinc does not colocalize
nocoloc_matrix = zeros(rows,cols);
nocoloc_histo = [];

for r = 1:rows
   for c = 1:cols
      % Check that the pixel is above threshold
      if cnx(r,c) >= thresh_cnx
         % If cnx is above threshold
         coloc_counter = coloc_counter + 1;
         coloc_intensity = coloc_intensity + vinc(r,c);
         coloc_matrix(r,c) = vinc(r,c);
         coloc_histo(end+1) = vinc(r,c);
      % If connexin is not at threshold but vinculin is, add to
      % non-colocalization threshold
%        elseif vinc(r,c) >= thresh_vinc
      else
         nocoloc_counter = nocoloc_counter + 1;
         nocoloc_intensity = nocoloc_intensity + vinc(r,c);
         nocoloc_matrix(r,c) = vinc(r,c);
         nocoloc_histo(end+1) = vinc(r,c);
      end
   end
end

dapi_counter = 0;
dapi_intensity = 0;
for r = 1:rows
   for c = 1:cols
      % Check that the pixel is above threshold
      if dapi(r,c) >= thresh_dapi
         % If cnx is above threshold
         dapi_counter = dapi_counter + 1;
         dapi_intensity = dapi_intensity + dapi(r,c);
      end
   end
end

Result.coloc_pxl = coloc_counter;
Result.coloc_total = coloc_intensity;
Result.nocoloc_pxl = nocoloc_counter;
Result.nocoloc_total = nocoloc_intensity;
Result.avg_coloc = coloc_intensity/coloc_counter;
Result.avg_nocoloc = nocoloc_intensity/nocoloc_counter;
Result.coloc = coloc_matrix;
```

```
Result.nocoloc = nocoloc_matrix;
Result.vinccoloc = Result.avg_coloc/dapi_intensity;
Result.vincnocoloc = Result.avg_nocoloc/dapi_intensity;
```

Ventricular rat cardiomyocyte isolation

Prior to isolation, rats were euthanized by carbon dioxide asphyxiation. The heart was excised and washed in sterile Buffer I (118 mM NaCl, 4.7 mM KCl, 1.3 mM KH_2PO_4, 1.25 mM $MgSO_4$, 1.2 mM $CaCl_2$, 15 mM HEPES, 16 mM glucose, pH 7.35) (*24*) at 37°C. The atria, right ventricle, and septal wall were removed and the left ventricle was washed 3X in sterile Buffer II (49 mM NaCl, 69 mM LiCl, 1.2 mM KH_2PO_4, 3.2 mM $MgSO_4$, 0.1 mM $CaCl_2$, 15 mM HEPES, 16 mM glucose, 60 mM taurine) for 1 min at 37°C. LV tissue was then minced and washed 3X in Buffer II for 5 min. Separated whole LV tissue was placed in either Trizol, mRIPA, or liquid nitrogen and transferred to -80^{o}C. Approximately 0.1 g of tissue was reserved and incubated at 37°C in 1 ml digestion buffer (Buffer II + 0.05% w/v collagenase + 1.5% w/v bovine serum albumin). After 15 min, the supernatant was discarded and the tissue, placed again in fresh digestion buffer, and incubated. After each 15 min interval, supernatant was reserved and 1 ml cardiomyocyte media (20% fetal bovine serum, 1% antibiotic/antimycotic in αMEM) was added to inhibit collagenase. Cardiomyocytes were then allowed to settle by gravity in 37^{o}C incubator for 1 h. Finally, the supernatant was discarded and the pellet was washed in 4^{o}C PBS and flash-frozen in liquid nitrogen.

Western blot analysis

Cell and tissue specimens were lysed with mRIPA buffer (50 mM HEPES pH 7.5, 150 mM NaCl, 1.5 mM $MgCl_2$, 1% Triton X-100, 1% Na-DOC, and 0.1% SDS) with 1 mM ethylene glycol tetraacetic acid (EGTA), 1 mM Na_3VO_4, 10 mM $Na_4P_2O_7$, and 1 mM phenylmethanesulfonylfluoride for Western blots. Concentration of ventricular cardiomyocyte proteins was measured via spectrophotometry. Each sample was then diluted to equal concentrations in mRIPA. Equal mass from each animal (6 mo or 24 mo) was pooled together. Western blotting analysis was performed with approximately 1 μg of protein per lane with three replicates per age. Ten percent polyacrylamide gels were

used for protein electrophoresis at 150 V for 1 hour until proteins were separated. They were subsequently transferred to polyvinylidene fluoride membranes (Bio-Rad) to be run at 100 V for 75 minutes in the transfer apparatus (Bio-Rad). The membranes were washed in Buffer A (25 mM Tris-HCl, 150 mM NaCl, and 0.1% Tween-20) and 15% milk overnight at 4°C and then incubated for 2 hours with the following antibodies: Vinculin (V9131) at 1:10,000 (Sigma Aldrich) and GAPDH (MAB374) at 1:2500 (Millipore). After three 10-minute washes with Buffer A, appropriate secondary HRP-tagged antibodies (Bio-Rad) were used during a 30 min incubation. After washing, immunoblots were visualized using ECL reagent (Thermo Fisher). Vinculin expression from Western blots were quantified from comparing three technical replicates of six pooled biological replicates at each age and normalizing to GAPDH intensity.

Drosophila microsurgeries

Preparation of the *Drosophila* heart for ventral imaging and atomic force microscopy (AFM) was performed as previously described (*22-24*). Adult female flies are first anesthetized with FlyNap (Carolina Biological) or with brief exposure to 5 – 10 psi CO_2 (<1 min) and then immobilized in 35-mm Petri dishes. The beating heart was ventrally exposed via microsurgery. Incisions are made to remove the head, thorax, and ventral abdominal cuticle. Flies are then submerged in oxygenated hemolymph at 25^{o}C. All organs and debris above the heart are excised with careful micropipette aspiration. Direct perturbation of the heart can result in a hypercontractile state resembling tetanus and activation of stretch-activated channels. Therefore all precautions were taken to not mechanically perturb the heart. All experiments are performed within 1 h of microsurgery although hearts were still beating and could maintain rhythmic contraction for up to 8 h if supplied with well-oxygenated hemolymph. Microsurgery did not influence fractional shortening or heart shortening velocities, an index of relative force production (fig. S7).

AFM-based nanoindentation

All indentation was performed with an MFP-3D Bio Atomic Force Microscope (Asylum Research) mounted in a Ti-U fluorescent inverted microscope (Nikon Instruments) with 2 μm-radius borosilicate glass beads mounted on 120 pN/nm silicon nitride cantilevers

(Novascan Technologies). All probes were calibrated for precise spring constant using the thermal noise method. All force curve analyses were performed by automated software custom-written in MATLAB (MathWorks) to calculate elastic modulus (in Pascals) of a local region of the myocardium within the heart tube as described previously (*24*). Microsurgery-prepped fly hearts were mounted on the AFM stage in a Fluid Cell Lite coverslip holder with 1 ml of oxygenated hemolymph. Immediately before indentation, normal rhythmic heart contraction is visually confirmed to ensure that tissue was not perturbed by the surgical procedure. The heart is then arrested by incubation in hemolymph containing 10 mM EGTA, resulting in chelation of free calcium, cessation of beating, relaxation of the heart tube, and opening of the ostia or inflow tracts. One-μm^2 area "force maps" were obtained with a 4 × 4 grid of indentations and an indentation velocity of 1 μm/s. Three "force maps" were obtained per animal, at 0, 15, and 30 μm from the ventral midline. Zero μm is proximal to the intercalated discs whereas 15 and 30 are considered ventral to the costameres or cortex.

Pharmacologically treated hearts were first indented in hemolymph containing EGTA at the ventral midline, proximal to the intercalated discs or cell-cell junctions, as well as 30 μm distally. Each heart was washed with fresh hemolymph and contractile recovery confirmed. Hearts were then incubated in hemolymph containing either 100 μM blebbistatin (Cayman Pharmaceuticals) or 100 μM cytochalasin D (Sigma). Indentation was repeated after 60 min. In the case of cytochalasin D–treated hearts, EGTA is added to induce a low-Ca^{2+} state. Contraction recovery through UV-inhibition of blebbistatin was confirmed 2 h after initial incubation. Hearts were capable of shortening under cytochalasin D treatment for up to 60 min.

Gene expression analysis

RNA was extracted from whole, beating heart tubes cleared of all non-muscle tissue debris using Zymo Research Quick-RNA Microprep Kit. RNA concentration and purity was quantified via spectrophotometry. Reverse transcriptase to synthesize first strand cDNA was performed from equal quantities of RNA per sample. For quantitative PCR, each reaction was run with 1 μl template cDNA, 2.5 μl forward primer, 2.5 μl reverse primer, 6.5 μl DEPC water, and 12.5 μl SYBR-green intercalating dye for a final reaction

volume of 25 µl. One biological replicate was considered to be 10 pooled hearts. Each gene was analyzed for at least three biological replicates per genotype and age and absolute quantity was calculated by comparison to a standard curve. Values are reported as absolute quantity or normalized geriatric/juvenile quantity or transgenic/control quantity. The primers were used for *Drosophila* are listed in table S13.

***Drosophila melanogaster* RNAi lines**

UAS-transgene fly lines were obtained from the Bloomington Drosophila Stock Center (BDSC), Vienna Drosophila RNAi Center (VDRC), or the Fly Stocks of the National Institutes of Genetics (NIG): UAS-Vinc gain-of-function line (BDSC stock No. 21870, 17482), UAS-Vinc RNAi (VDRC stock No. 34568), and UAS-MHC RNAi (NIG stock No. 17927R-1). The cardiac tissue–specific tinHE-Gal4 (*tinman* heart-enhancer) driver and *FM6;Sco/CyO* balancer lines were generous gifts from Georg Vogler (Sanford-Burnham Medical Research Institute, La Jolla, CA). For both RNAi silencing or overexpression/gain-of-function, UAS-transgenic males were crossed with virgin female tinHE-Gal4 flies and maintained at 25˚C throughout all life stages. Newly eclosed female progeny were isolated into separate vials with identical culture conditions. Food was changed every fourth day. All experiments were performed on these females at their appropriate age.

Immunofluorescent labeling of the fly heart

Briefly, ventrally-exposed beating hearts were treated with 10 mM EGTA, then with 3.7% paraformaldehyde in hemolymph, and then permeabilized in 0.1% Triton X in PBS (PBST). Samples were blocked with 1% ovalbumin in PBST before being incubated in primary antibody overnight at 4°C. Samples were then washed and blocked with ovalbumin for 60 min. Heart tubes were submersed in secondary antibodies in PBST, washed with PBST and then PBS before mounting on 25-mm coverslips with Fluoromount. Fluorescent microscopy was performed on a Ti-U fluorescent inverted microscope with CARV2 confocal controller and CoolSnap HQ CCD camera.

Fly heart preparation for transmission electron microscopy imaging

Dissections were performed as described previously (*30*). Preparation of the heart for transmission electron microscopy (TEM) began with microsurgery, as with AFM and immunofluorescence. Proper heart contraction was visually confirmed at 60X. Hearts were then relaxed with 0.01 M EGTA in artificial hemolymph and washed 3x with PBS. The samples were then fixed overnight at 4ºC or on ice in 2 ml of primary fixative (3% formaldehyde, 3% glutaraldehyde in 0.1 M cacodylate buffer, pH 7.4). Samples could be stored in primary fixative for several weeks. Once fixed, a wash step was performed 6X for 5 min each with 2 ml 0.1 M KPO_4 buffer (pH 7.2) on ice. A secondary fix was performed on ice in the dark for 2 h using 2 ml of fresh secondary fixative solution (1% OsO_4, 100 mM phosphate buffer, and 10 mM $MgCl_2$, pH 6.0). Samples were washed 3X for 5 min each with 2 ml H_2O. All subsequent steps before polymerization were performed at room temperature. After secondary fixation, samples were block stained with aqueous 2% uranyl acetate at room temperature, left overnight in the dark, and then washed 3X for 5 min each with 2 ml H_2O. An acetone dehydration series were then performed at 30 min each: 25%, 50%, 75%, 95%, and 3X 100% anhydrous acetone.

Samples were embedded in fresh Epon plastic mix (16.2 ml EM bed-812 Epon 812 substitute), 10.0 ml dodecenyl succinic anhydride, 8.9 ml NMA, 0.5-0.7 ml 2,4,6-Tn(dimethylamino)phenol. Samples were treated with 1:1 Epon mix and 100% anhydrous acetone, then 3:1 Epon mix and 100% anhydrous acetone, for 30 min each. Finally, they were submerged in 100% Epon mix at room temperature. Samples were oriented and embedded in Epon-filled BEEM capsules and polymerized at 60°C for 1 day. Thin sections (40-70 nm) were sliced from the embedded samples using a Diatome diamond knife and mounted on grids coated with formvar. Each slice was then stained with 2% uranyl acetate for 30 min and Sato's lead stain for 1 min. To make Sato's lead stain, add 1 g lead nitrate, 1 g lead citrate, 1 g lead acetate, and 2 g sodium citrate were added to 82 ml distilled H_2O and mixed; then, 19 ml of 4% NaOH was added. The solution was mixed, filtered through #1 filter paper, and stored in the dark at 4°C. Finally, images were obtained at 120 kV on a FEI Tecnai 12 Transmission Electron Microscope.

TEM imaging and analysis

Measurement of average distance between adjacent thick filaments and interfilament spacing was performed with a custom-written MATLAB script (fig. S14). For this procedure, the original image is first imported into ImageJ in order to remove background to minimize grain noise. In order to locate thick and thin filaments, the grey-scale image was inverted such that filaments appeared bright on a dark background. A mask was created from the thick filaments by thresholding images above a given brightness and within a specified particle range that excludes thin filaments and large, non-filamentous objects. Centroids for each isolated thick filaments were recorded and average thick-thick filament distance was calculated by measuring the average distance to all adjacent thick filaments for each thick filament. The isolated thick filament image was then used as a mask to isolate thin filaments in the original image. A similar algorithm was used to isolate thin filaments: thresholding by brightness and object or particle size and then calculating centroids. Each thin filament was then associated with its most proximal thick filament. For each thick filament, the average distance to all its associated thin filaments was computed using a strategy outlined in fig. S14. F-test was performed on 480 and 670 thick filaments from control and *VincHE* flies, respectively.

SUPPLEMENTAL FIGURES

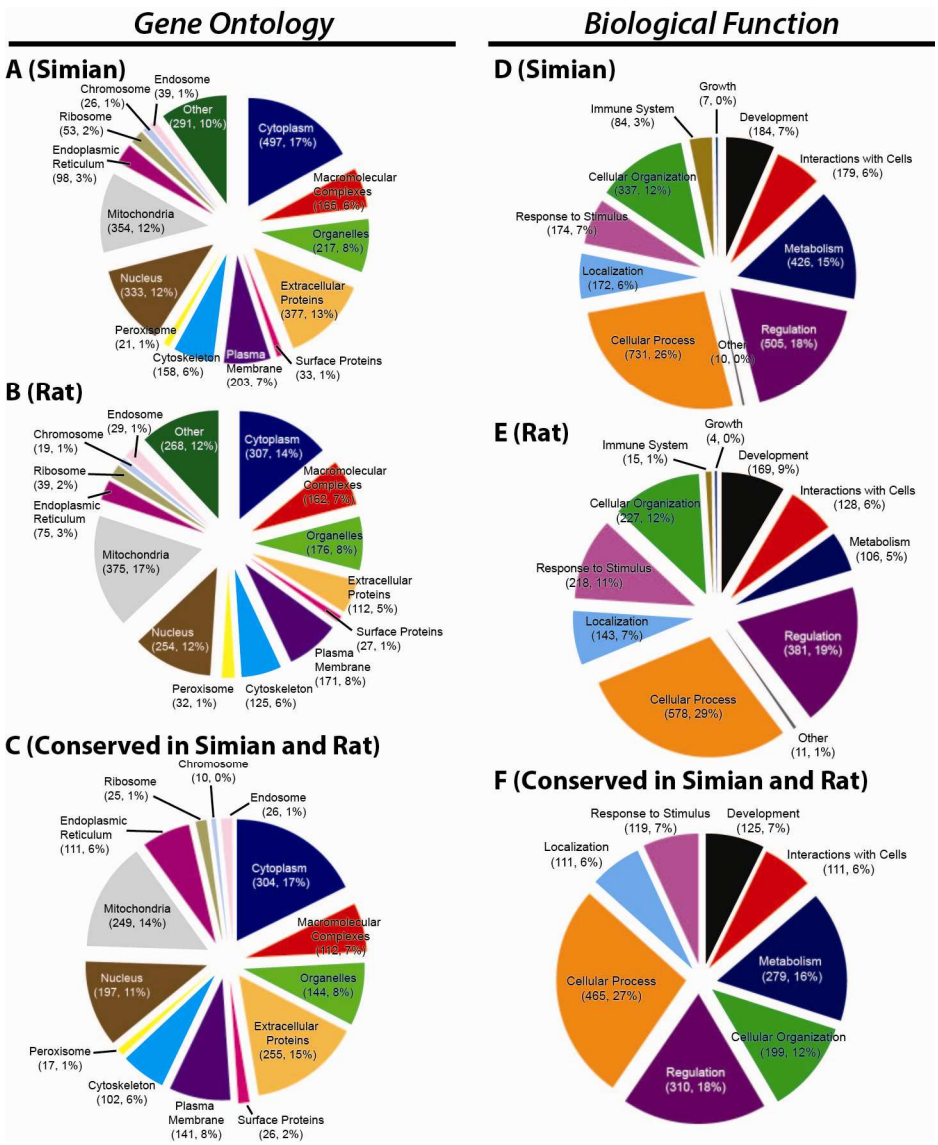

Fig. S1: STRAP analysis of gene ontology and biological function for simian and murine proteomes. Proteins were identified using mass spectrometry and quantified based on normalized spectral counts (tables S3-S4). (**A** and **B**) Proteins from simian and murine left ventricles based on gene ontology. (**C**) Conserved murine and simian proteins clustered by ontology (n = 602). (**D** and **E**) Proteins from simian and murine left ventricles based on biological function. (**F**) Conserved proteins clustered by biological function. Data expressed in parentheses reflect the number of proteins detected for the indicated ontological term and its percentage of the total number of proteins detected. GO and biological function were assigned by STRAP software allowing multiple ontological terms to be mapped to an individual protein.

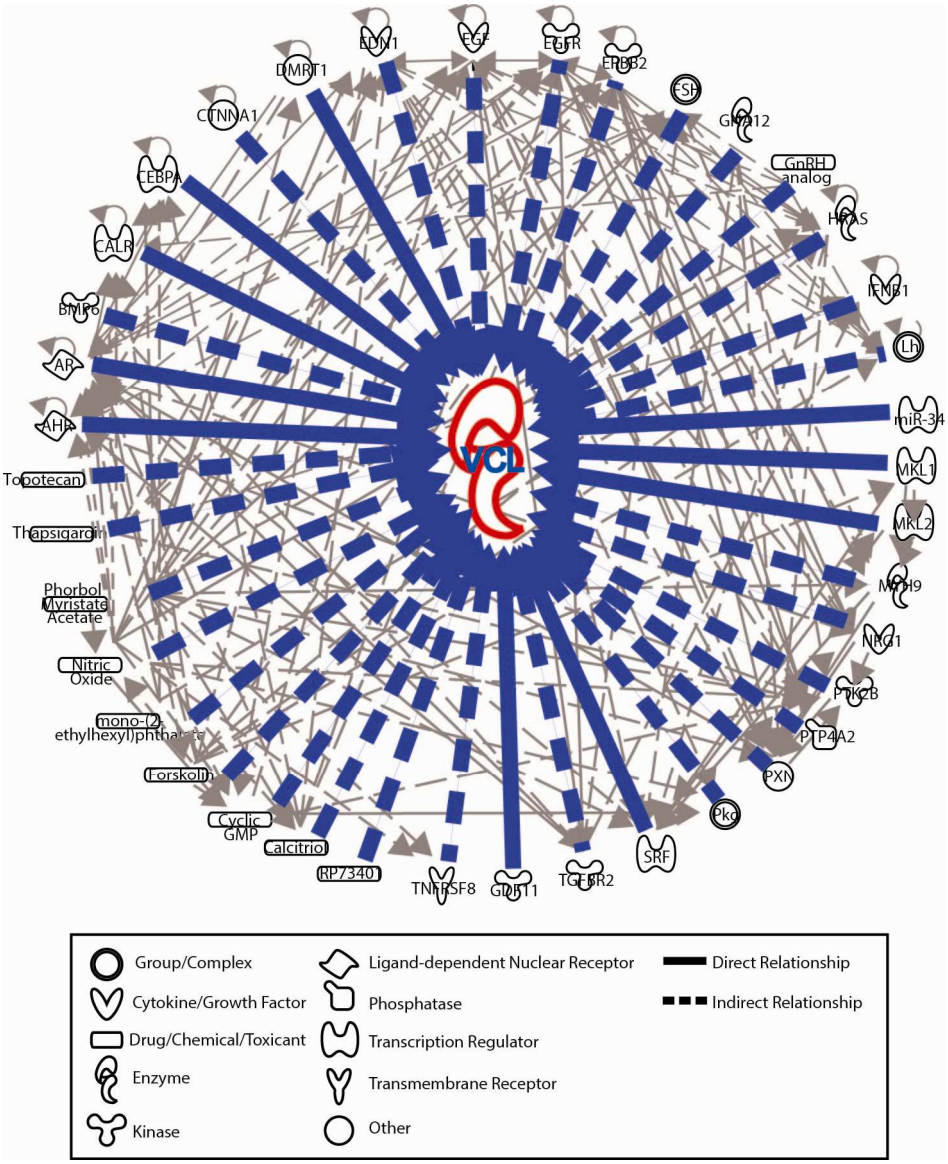

Fig. S2: Partial interaction map of upstream vinculin regulators. IPA is shown for potential interventional or therapeutic proteins and drugs that act on vinculin. Specific vinculin interactions are in bolded blue.

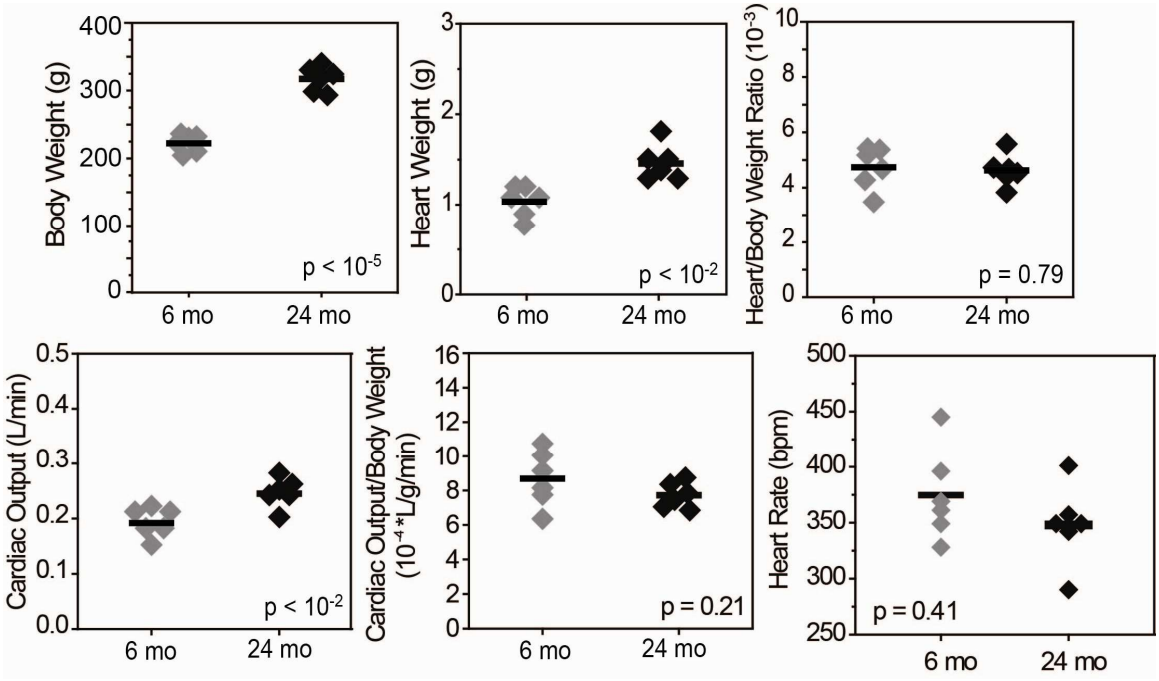

Fig. S3: Biometric comparison of adult and aged rats. Body weight (BW), heart weight (HW), ratio of HW/BW, cardiac output (CO), ratio of CO/BW, and heart rate were all assessed for adult and aged rats. Data are individual animals and mean (n = 6 per time point). P-values determined using non-parametric t-tests.

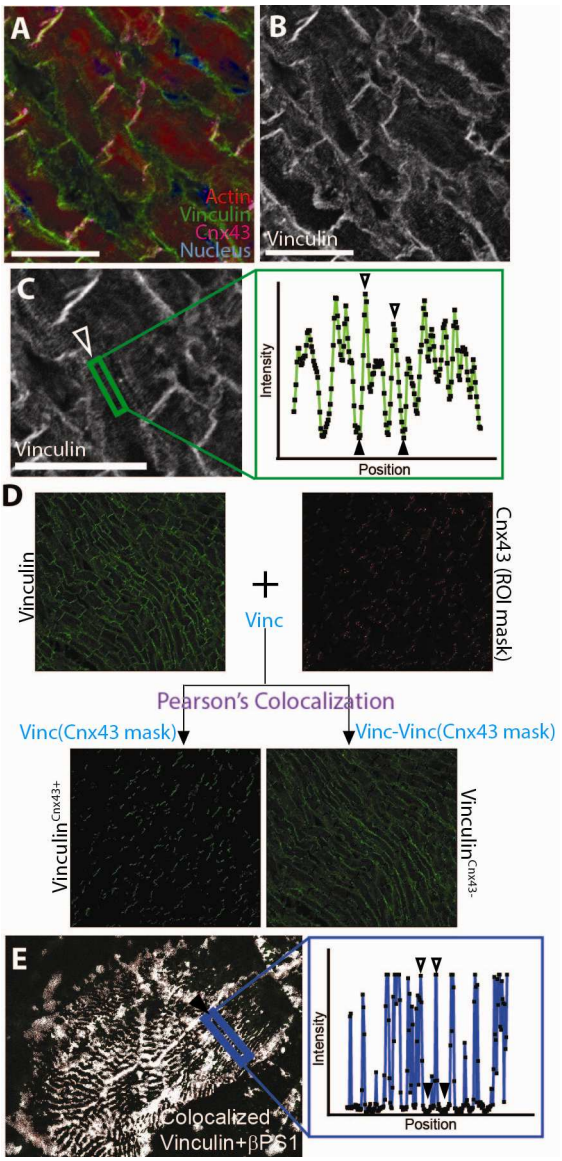

Fig. S4: Analysis of vinculin localization in rat and fly myocytes. (**A**) Magnified image of 24 mo rat tissue labeled for actin, vinculin, connexin 43 (Cnx43), and nuclei. (**B**) Vinculin channel of the merged image in (A). (**C**) Magnified image the of vinculin channel in (A) with a line plot indicating periodic increases in intensity along the length of the green box (open and closed arrowheads indicate local peak and minimum intensities, respectively). (**D**) Cnx43 was used as a mask to discriminate vinculin at the ID versus costameres (top). Pixels were separated by colocalization analysis algorithm in FIJI, which is based on the Pearson's colocalization coefficient analysis (middle). Total vinculin was separated into Cnx43-localizing ($Cnx43^{+}$) and all else ($Cnx43^{-}$). Integrated density was computed from each image for each animal and normalized to DAPI (bottom). **(E)** Vinculin and β1-integrin co-localization in *Drosophila* heart. The line plot indicates intensity over the long axis of the blue box (open and closed arrowheads indicate local peak and minimum intensities, respectively). Periodicity indicates striations from costameric labeling by vinculin and β1. Scale bars in (A to C), 10 μm.

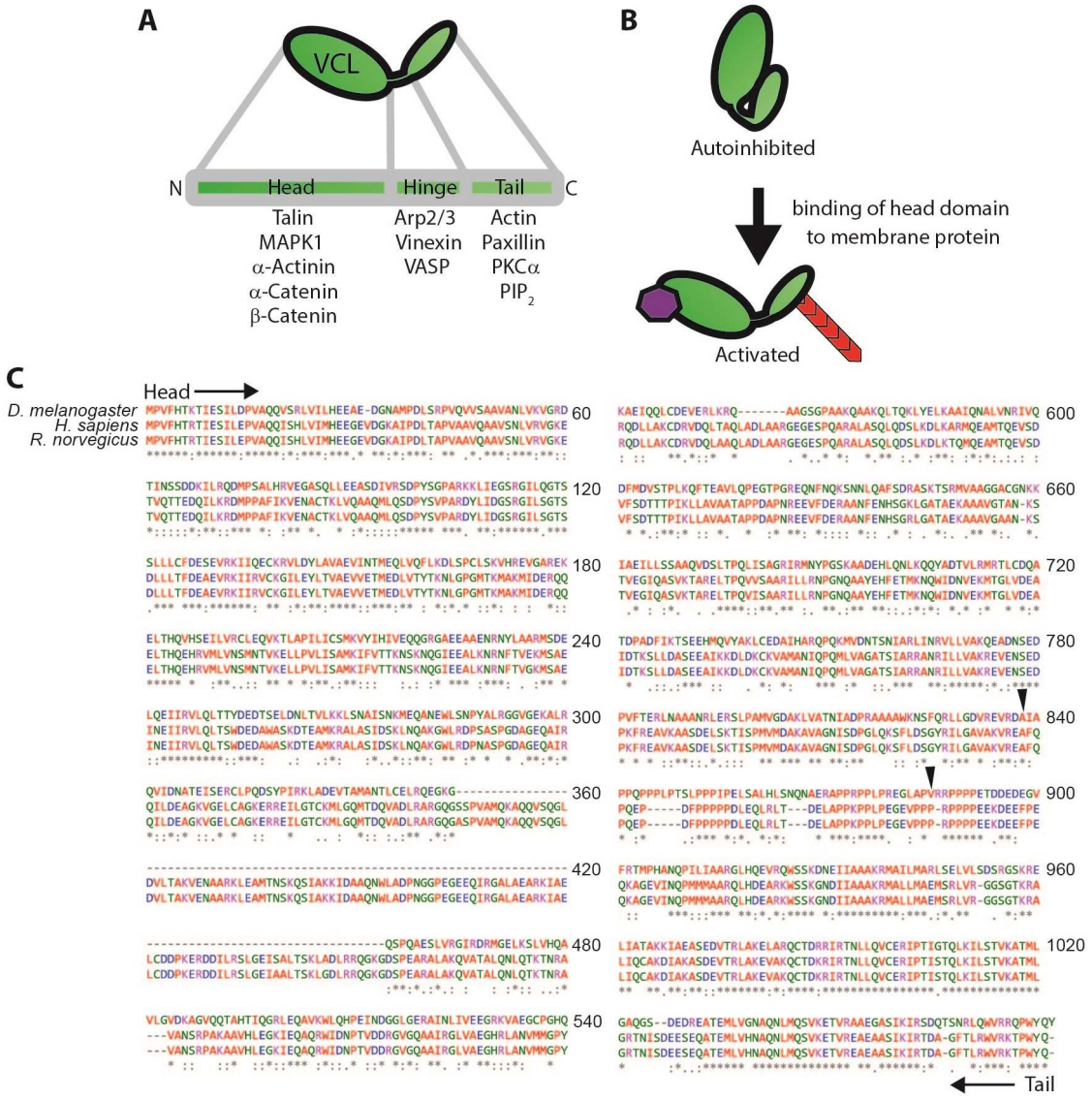

Fig. S5: Vinculin structure and homology across monkey, rat, and fly. (**A**) Cartoon structure of vinculin's head, hinge, and tail domain, with annotations for protein binding to each section. (**B**) Schematic of vinculin activation. (**C**) Sequence alignment for vinculin for the indicated species. Head and tail domains are indicated with arrowheads pointing out the hinge domain. Matched and missing amino acids are indicated by gray asterisks and dashes, respectively. Mismatched amino acids with close charge or polarity are indicated with gray dots.

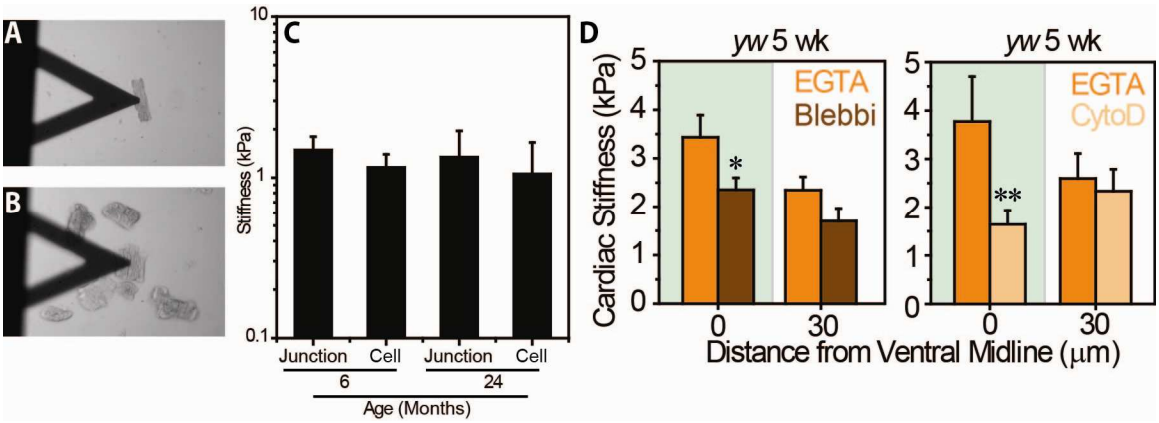

Fig. S6: Indentation of isolated adult and aged rat cardiomyocytes and intact fly hearts. (**A**) Bright field image of an AFM cantilever on top of an adult rat 6 month LV myocyte plated on type I collagen. (**B**) AFM cantilever positioned over the cell-cell junction of two rat myocytes for indentation of the region containing the intercalated disc. There was poor adhesion after 24 h in culture when measurements were made. (**C**) Stiffness measurements of isolated adult and aged rat cardiomyocytes at the indicated positions within the cells. Data are means ± SD (n = 10 per age and location). Data were not statistically significant versus each other, as assessed by t-tests. (**D**) *Drosophila* cardiac stiffness as a function of drug treatment at the midline (0 μm) and 30 μm distal to the midline in 5-wk *yw* flies. Absolute stiffness is plotted with respect to the indicated treatment. Data are means ± SD (n = 10 per treatment and location) *P < 0.05, **P < 0.01 versus EGTA at the respective distance, one-way repeated measures ANOVA.

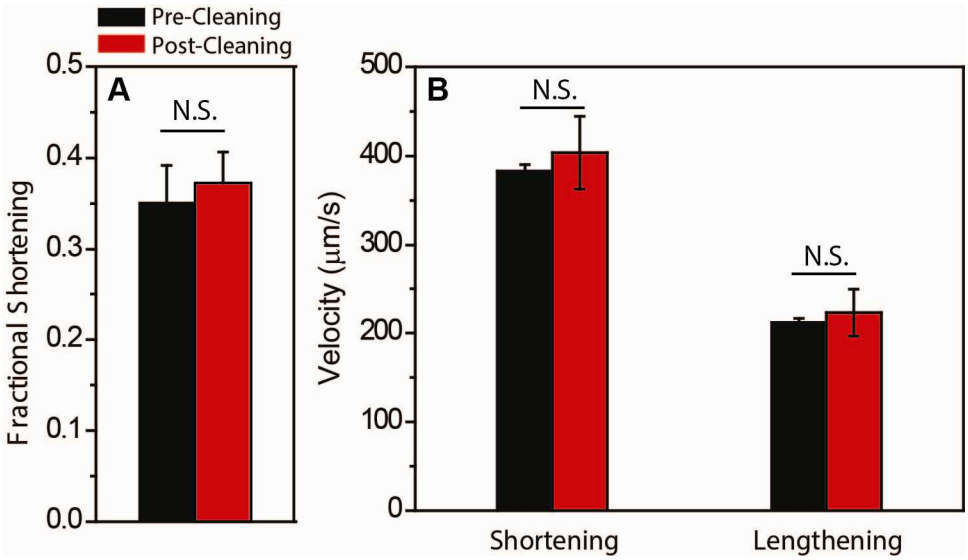

Fig. S7: Effects of heart tube preparation on its function. Fat or fibrous tissue deposits were removed from the top of the *Drosophila* heart to ensure contact only with muscle. Fractional shortening and wall velocities were measured before and after the extensive cleaning performed on intact hearts. Data are means ± SD (n = 10). N.S., no statistical difference determined by paired t-tests.

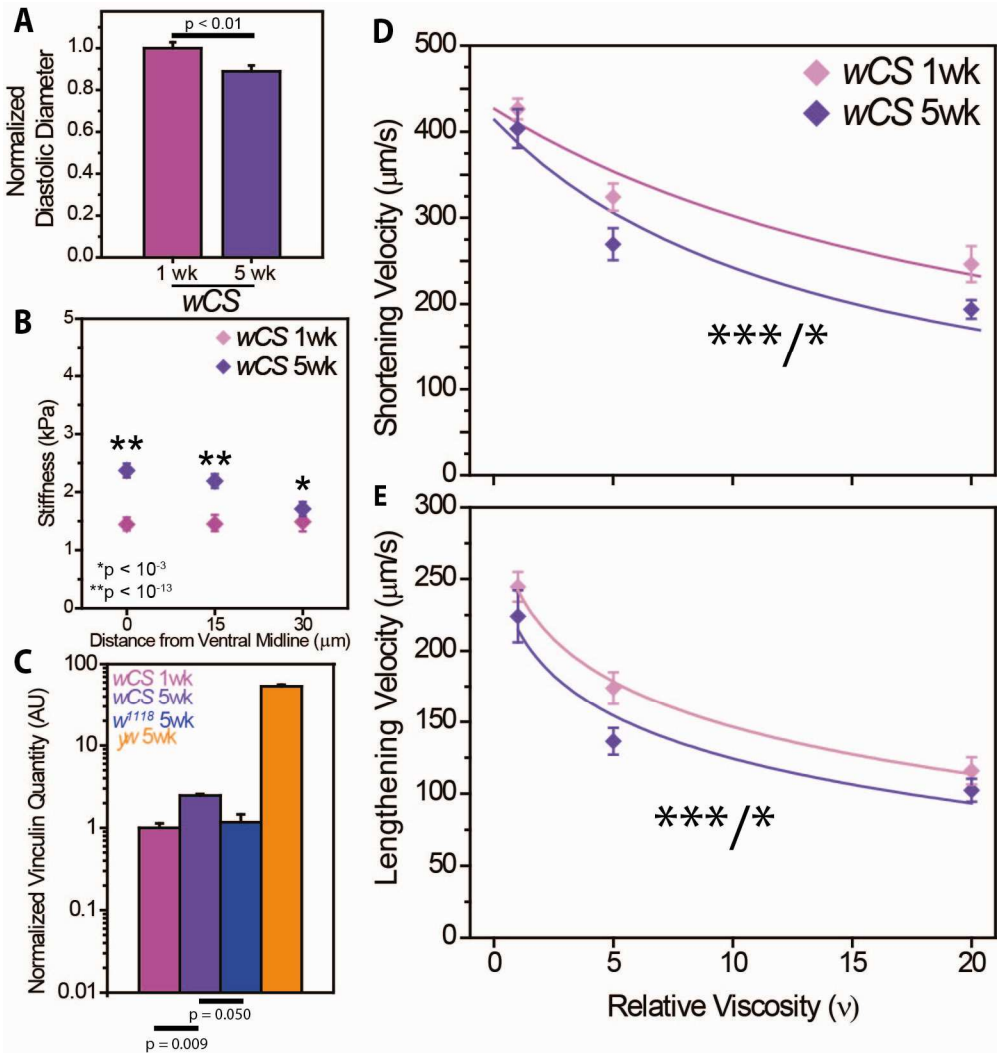

Fig. S8: Characterization of diastolic diameter, cardiac stiffness, and vinculin expression in the *wCS* *Drosophila* genotype. Age-associated decline in diastolic diameter (**A**) and cortical stiffening (**B**) for *white-Canton S* (*wCS*) flies of indicated age. Data are means ± SEM ($n > 15$ per age). *$P < 0.05$, **$P < 0.01$, one-way ANOVA. (**C**) *Vinculin* expression as a function of age in three different *Drosophila* genotypes. Data are means normalized to 1-wk *wCS* ± SEM ($n = 3$ biological replicates with 10 pooled hearts). *P*-values determined using one-way ANOVA. (**D** and **E**) Shortening velocity and lengthening velocity were not significantly reduced in unloaded conditions. Data are means ± SEM ($n > 20$). Hill's fit is shown for shortening velocity. Log-fit is shown for lengthening velocity for illustrative purposes. *$P < 0.05$ and ***$P < 0.001$, where asterisks to the left and right indicate *P*-values from two-way ANOVA for difference in velocity between viscosity and age, respectively (e.g. ***/* indicates $P < 0.001$ for reduction in velocities as a function of load, and $P < 0.05$ for difference in velocity profile between *wCS* 1- and 5-wk.

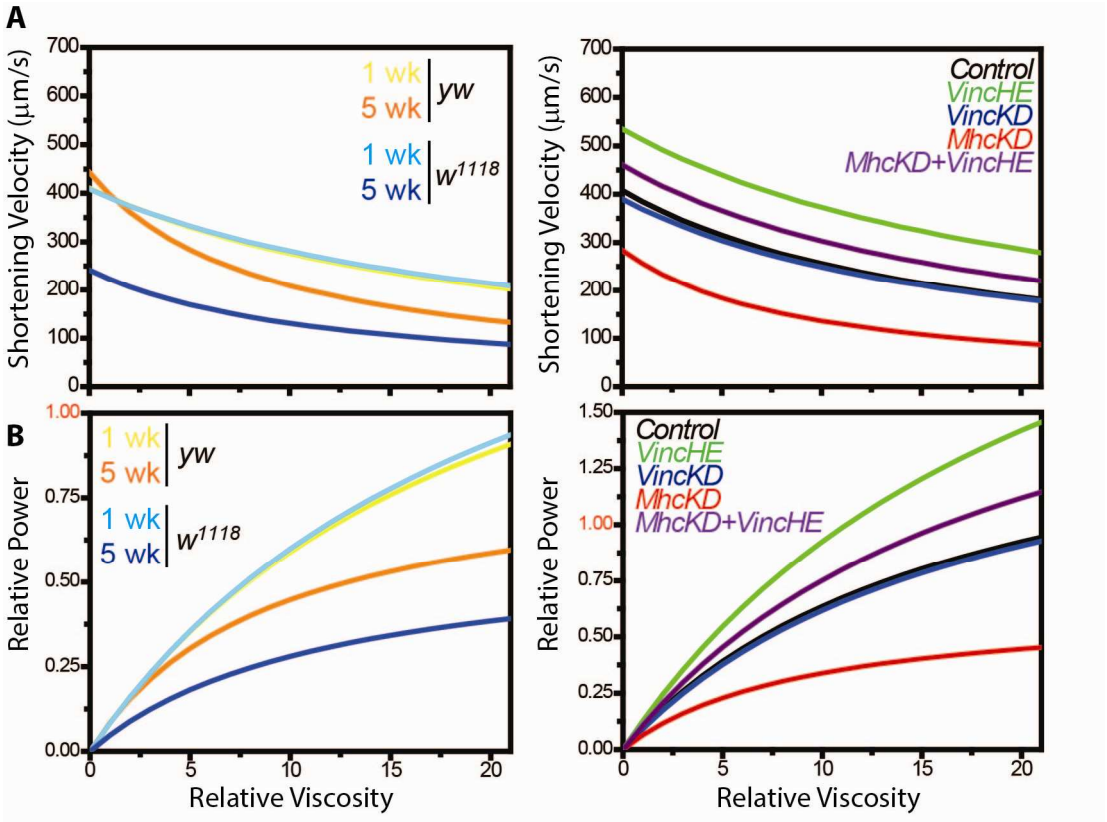

Fig. S9: Fitting shortening velocities with Hill's muscle model. (**A** and **B**) Least-squares fit to Hill's muscle for shortening velocity (A) and relative power output (B) as a function of relative viscosity for 1- and 5-wk wild-type flies and 1-wk cardiac-specific mutant flies (*VincHE*, *VincKD*, *MhcKD*, and *MhcKD+VincHE*). Relative power output was normalized to 1-wk w^{1118} (left panels) and 1-wk Control (right panels).

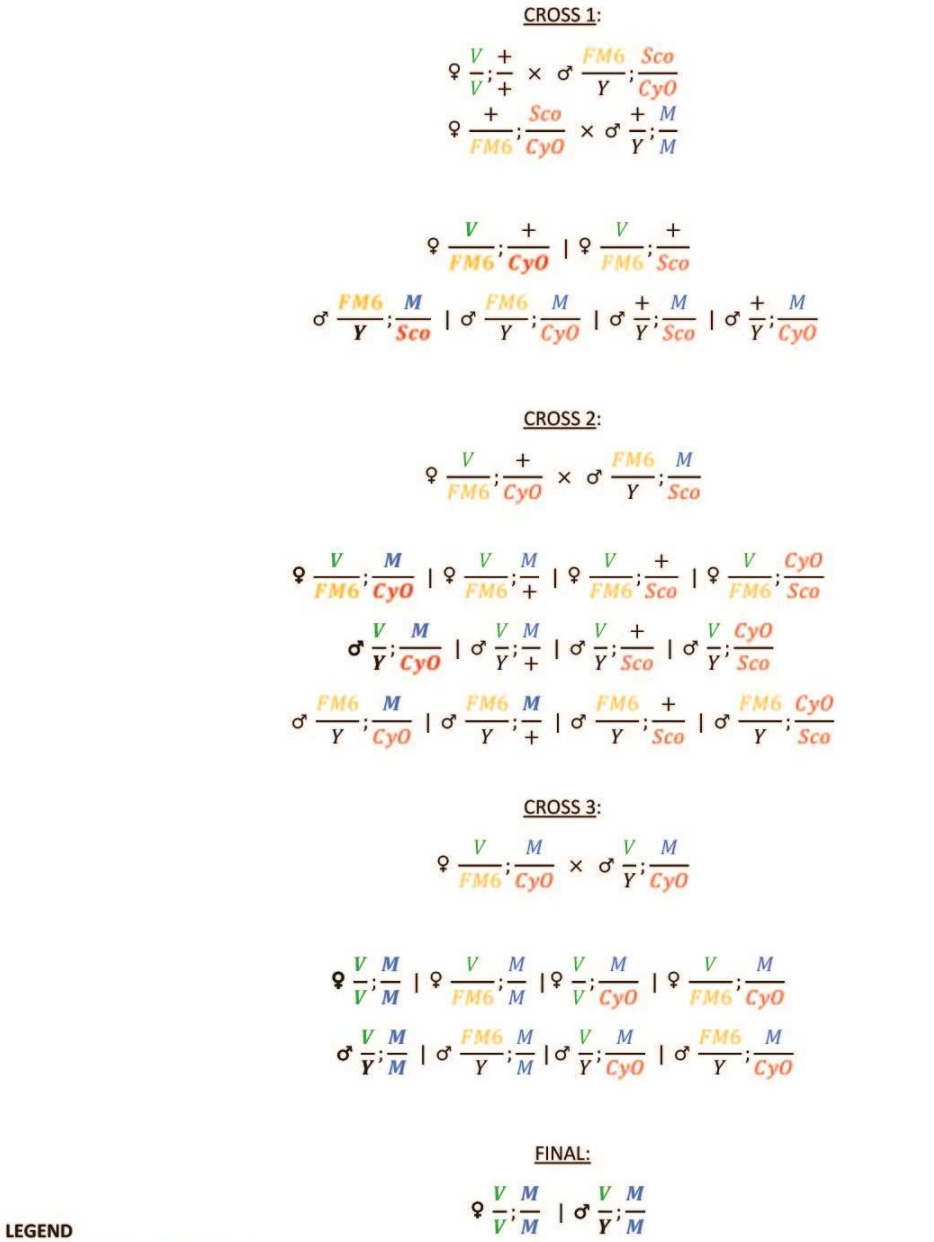

Fig. S10: Generation of the UAS-Mhc RNAi;UAS-Vinc line. The illustration outlines the series of crosses that were performed in order to create a line that was homozygous for both UAS-MHC RNAi (on chromosome II) and UAS-Vinc (on the autosomal/X chromosome). FM6/Y;Sco/CyO (X;II) was used as a balancer (FM6 on X and Sco or CyO on II). Progeny from each cross that were selected for breeding are shown in bold.

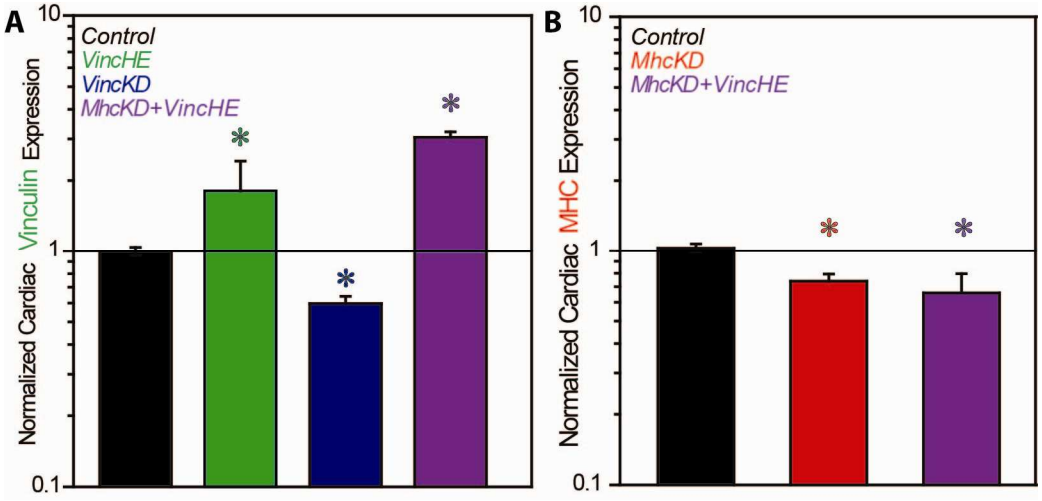

Fig. S11: Quantification of genetic perturbations in *Drosophila* hearts. (**A**) Overexpression of *Vinculin* in 1-wk *VincHE* and *MhcKD+VincHE* as well as knockdown in 1-wk *VincKD* flies. (**B**) *Myosin heavy chain* (MHC) knockdown in *MhcKD* and *MhcKD+VincHE* by heart-specific qPCR. Data are means ± SD (n = 3 biological replicates with 10 pooled hearts). Data are absolute quantities of transcript normalized to control (1-wk female progeny of *tinHE-Gal4* × w^{1118}). *P < 0.05 compared to control, one-way ANOVA.

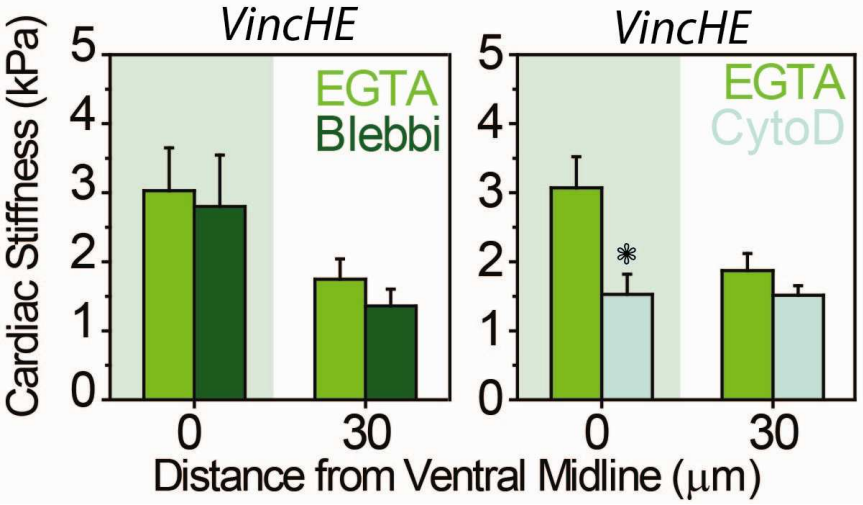

Fig. S12: Change in *VincHE* stiffness with cytoskeletal perturbation. Average stiffness is shown per drug treatment at the midline (0 μm) and 30 μm distal to the midline in *VincHE* flies. Average stiffness ± SD (n = 10) is plotted with respect to the indicated blebbistatin or cytochalasin D treatment for 30-60 min. *P < 0.05 versus EGTA-treatment at respective location, one-way ANOVA.

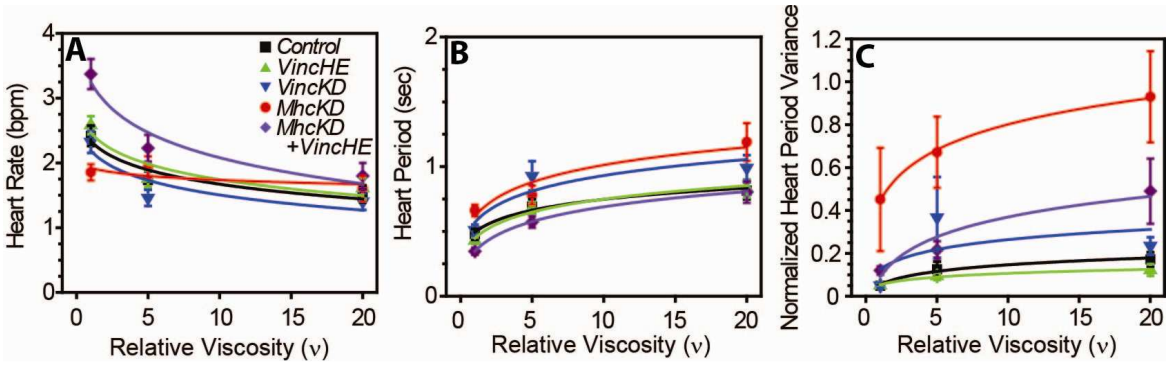

Fig. S13: Transgenic fly heart rate, period, and rate variance. (**A**) Heart rate in beats per minute (bpm). (**B**) Heart period, the time taken for systole and diastole, in s. (**C**) The normalized heart period variance, an index of rhythmicity (greater variance indicates impaired rhythmicity). Data are means ± SEM (n > 29), for all *Drosophila* transgenic genotypes in Fig. 6. Indices did not differ between *VincHE* and control (P > 0.05, comparing each metric as a function of load using two-way ANOVA). Log-fits shown for illustrative purposes.

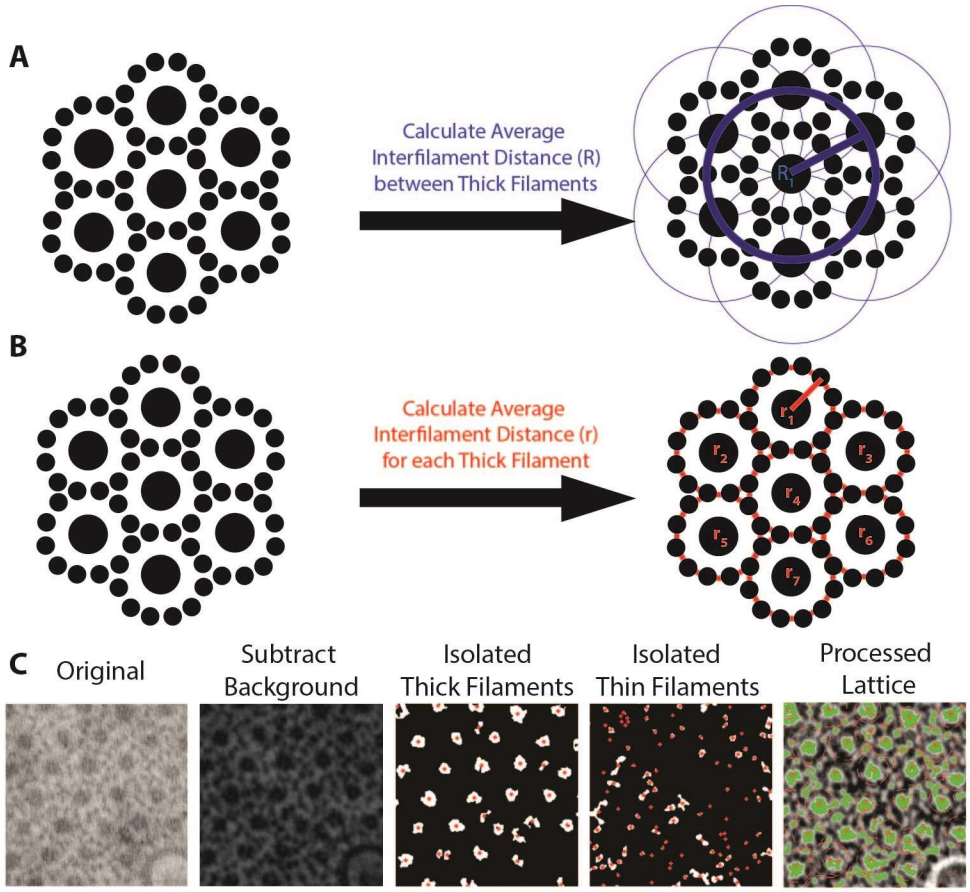

Fig. S14: Analysis of interfilament spacing in TEM images from the *Drosophila* heart. Custom-written particle-tracking algorithms were used to process TEM images of the cardiac myofilaments in cross-section. (**A**) Thick-thick interfilament spacing (*R*) was reported as the average distance between the centroid of each thick filament and the centroid its nearest thick filament neighbors. (**B**) Thick-thin interfilament spacing (*r*) was reported as the average distance between each thick filament centroid and the centroids of its nearest thin filament neighbors. (**C**) Micrographs were processed to subtract background noise, isolate thick and thin filaments based on size, and then have centroids calculated and highlighted.

SUPPLEMENTAL TABLES

Table S1: Peptides detected by mass spectroscopy for adult and aged rhesus monkey left ventricles. Peptides, including those that were modified, were detected by mass spectrometry in adult and aged samples of left ventricles of *Macaca mulatta*. Data include each peptide's spectral count, the protein ID to which the peptide was mapped, and a description of that protein. Peptide charge, observed and calculated mass (and its difference), and the probability that the predicted peptide is correct are also listed. Data represent total peptides detected over all samples (n = 9). Protein annotations were made with Ingenuity Pathway Analysis (IPA).

Table S2: Peptides detected by mass spectroscopy for adult and aged rat left ventricles. Peptides, including those that were modified, were detected as described in the Extended Methods for adult and aged samples of left ventricles of *Rattus norvegicus* and are listed here. Data include each peptide's spectral count, the protein ID to which the peptide was mapped, and a description of that protein. Peptide charge, observed and calculated mass (and its difference), and the probability that the predicted peptide is correct are also listed. Data represent total peptides detected over all samples (n = 12). Protein annotations were made with IPA.

Table S3: Proteomic analysis for adult and aged rhesus monkey left ventricles. Total spectral counts were assessed for adult (n = 4) and aged (n = 5) left ventricle samples. Protein group IDs and descriptions of *M. mulatta* were obtained by Software Tool for Rapid Annotation of Proteins (STRAP) and provided alongside peptide probability assessments. Aged/adult ratio of spectral counts is shown and was used in subsequent IPA. [#]Proteins only expressed in the aged population.

Table S4: Proteomic analysis for adult and aged rat left ventricles. Total spectral counts were assessed as described in the Extended Methods for adult (n = 6) and aged (n = 6) samples of left ventricle. Protein group IDs and descriptions of *R. norvegicus* were obtained by STRAP and fit to data and probability assessments provided. Aged/adult ratio of spectral counts is shown and used in subsequent IPA. [#]Proteins expressed only in the aged population.

Table S5: STRAP annotation of the cellular compartments of the proteins detected in both rat and monkey proteomes. Analysis of 602 proteins conserved in the left ventricles across all species and ages, and the cellular compartments that map to those proteins. Note that multiple ontologies, as obtained by STRAP, exist per protein. Proteins may have additional, undiscovered ontological functions.

Table S6: STRAP annotation of biological functions for rat and monkey. Analysis of 602 proteins conserved in the left ventricles across all species and ages and the biological function ontologies, obtained by STRAP, that map to those proteins. Note that multiple ontologies exist per protein.

Table S7: IPA of bio-function expression for rat. Most well-represented IPA Bio-functions ($P < 0.05$) from comparative analysis of adult and aged rat left ventricles for intercalated disc, sarcomeric, and costameric genes. Significance computed by IPA is listed as –log(p-value) or a value of ≥1.3. Cardiovascular-related functions are indicated in bold. Vinculin is shown in italics and underlined.

Table S8: IPA of tox-function expression for rat. Most well-represented IPA Tox-functions ($P < 0.05$) from comparative analysis of adult and aged rat left ventricles for intercalated disc, sarcomeric, and costameric genes. Significance computed by IPA is listed as –log(p-value) or a value of ≥ 1.3. Cardiovascular-related functions are indicated in bold. Vinculin is shown in italics and underlined.

Table S9: IPA and OMIM annotation of age–up-regulated proteins associated with cardiac function. Proteins that were upregulated with age, including vinculin, are annotated. Annotations (for instance, cytogenetic location in *Homo sapiens*, or associated cardiomyopathies) were obtained from Online Mendelian Inheritance in Man (OMIM). The table included here only shows proteins with normalized count > 1 and whose mutation is associated with cardiomyopathy in humans based on OMIM classification. A complete set of proteins can be found in Supplementary Excel file "Table S9." # denotes proteins expressed only in the aged population.

Protein group description (Species: *Homo sapiens*)	Gene symbol	Normalized count (aged/adult)
Nexilin	*NEXN*	#
BAG family molecular chaperone regulator 3	*BAG3*	3.33
δ-Sarcoglycan	*SGCD*	2
Dystrophin	*DMD*	1.5
Desmoplakin	*DSP*	1.38
Telethonin	*TCAP*	1.33
α-Actinin-2	*ACTN2*	1.32
Troponin C, cardiac	*TNNC1*	1.32
Vinculin	*VCL*	1.32
Tropomyosin α-1 chain	*TPM1*	1.31
Myosin-7	*MYH7*	1.29
Myosin light chain	*MYL3*	1.26
Laminin α-4	*LAMA4*	1.25
Titin	*TTN*	1.22
Caveolin-3	*CAV3*	1.2
Cysteine and glycine-rich protein 3	*CSRP3*	1.2
LIM domain-binding protein 3	*LDB3*	1.2
Myosin binding protein C, cardiac	*MYBPC3*	1.18
Troponin T, cardiac	*TNNT2*	1.15
Troponin I, cardiac	*TNNI3*	1.14
αβ crystallin	*CRYAB*	1.13
Myosin regulatory light chain 2	*MYL2*	1.1
Myozenin-2	*MYOZ2*	1.05
Succinate dehydrogenase flavoprotein subunit	*SDHA*	1.01

Table S10: IPA of upstream regulators of age-related proteins identified in rat and simian. Database of upstream regulators (chemical, kinases, enzymes, transporters, transcriptional regulators, miRNAs) and their associated proteins identified in the aging proteomic analysis of monkeys and rats. Note that upstream regulators and associated proteins or pharmacological agents that affect expression are limited to annotations in the databases listed.

Table S11: Expression of candidate actin-binding molecules in *Drosophila* hearts using qPCR. Raw data of absolute transcript quantity (mg/ml) for indicated genes and genotypes. Ratios of aged to adult data are plotted as a heat map in Fig. 4E. Data are averages ± SEM ($n \geq 5$ biological replicates of more than 20 pooled hearts per sample).

Table S12: Fitting shortening velocities with Hill's muscle model. Coefficients for the Hill's muscle model equation for each genotype or age. Fit was applied to the average value of shortening velocity over all loads within each group.

Table S13: qPCR primers. *Drosophila* primers used for qPCR measurements of heart tube. Primers were designed by NCBI Primer Blast against sequences found on FlyBase. Note that the FN1 gene is used to generate a standard curve based on a human fibronectin plasmid.